



# Synthesis and photophysical studies of back-to-back dinuclear platinum terpyridine complexes with different substituents on the bridging ligand

Rui Liu<sup>a,b</sup>, Zhongjing Li<sup>a</sup>, Hongjun Zhu<sup>b</sup>, Wenfang Sun<sup>a,\*</sup>

<sup>a</sup> Department of Chemistry and Biochemistry, North Dakota State University, Fargo, North Dakota 58108-6050, United States

<sup>b</sup> Department of Applied Chemistry, College of Science, Nanjing University of Technology, Nanjing 210009, PR China

## ARTICLE INFO

### Article history:

Received 23 November 2011

Received in revised form 15 February 2012

Accepted 19 February 2012

Available online 25 February 2012

### Keywords:

Dinuclear platinum complex  
1,4-Bis(terpyridin-4-yl-vinyl)benzene  
Electronic absorption  
Emission  
Transient absorption  
Synthesis

## ABSTRACT

Four back-to-back dinuclear platinum terpyridine complexes with different substituents on the bridging ligand (**1a–1d**) were synthesized and characterized. Their electronic absorption, photoluminescence and triplet transient difference absorption were systematically investigated. All complexes exhibit strong <sup>1</sup>MLCT/<sup>1</sup>ILCT absorption bands in the visible region, which significantly red-shifts when electron-donating substituents are introduced on the conjugated bridge and blue-shifts when electron-withdrawing substituents are present. Excitation of **1a** and **1d** in solution at their respective low-energy absorption band at room temperature results in an orange and red luminescence, respectively, which can be tentatively attributed to the <sup>1</sup>MLCT/<sup>1</sup>ILCT excited state. These complexes exhibit intense broad triplet transient difference absorption in the visible to the near-IR region, which likely arises from the ligand-localized states (<sup>3</sup>π,π\* or <sup>3</sup>ILCT). Electron-donating substituent causes a pronounced red-shift, while electron-withdrawing substituents induce a blue-shift of the triplet transient absorption bands.

© 2012 Elsevier B.V. All rights reserved.

## 1. Introduction

Square-planar platinum(II) complexes have attracted great attention in the past two decades because of their interesting spectroscopic properties and potential applications in optoelectronic devices [1–5], chemosensors [6,7], photocatalysis [8–10] and nonlinear optical materials [11–14]. The square-planar Pt(II) coordination of these complexes reduces the  $D_{2d}$  distortion that is likely to result in radiationless decay process [3,5], which enhances the emission of these complexes. In addition, their photophysical properties can be modulated by structural modification of the ligands to meet the requirements for different applications. For example, the nature of the lowest excited state of these complexes can be tuned among the metal-to-ligand charge transfer (MLCT) state, ligand-to-ligand charge transfer (LLCT) state, intraligand charge transfer (ILCT) state, and intraligand (IL)  $\pi, \pi^*$  state depending on the nature of the ligand.

Among these, the photophysical properties of dinuclear platinum terpyridine complexes are more interesting by virtue of the possible intramolecular Pt–Pt and  $\pi$ – $\pi$  interactions in the dinuclear complexes, which could tune their electronic absorption and luminescence properties. Most of the earlier work reported on the dinuclear platinum complexes used a rigid bridging ligand

to form a face-to-face geometry, which possibly resulted in different degrees of metal–metal and  $\pi$ – $\pi$  interactions [15–18]. However, the studies on the dinuclear platinum terpyridine complexes with a back-to-back geometry are still very limited. Ziesel group [19] synthesized one back-to-back dinuclear platinum complex using a 1,4-diethynyl-2,5-didodecyloxybenzene as bridging ligand. Our group has reported the influence of conjugated rigid bridging ligands on the photophysics of the “back-to-back” dinuclear platinum complexes, which exhibit strong reverse saturable absorption (RSA) in the visible to the near-IR region for nanosecond laser pulses [12]. Meanwhile, to the best of our knowledge, the influence of the substituents on conjugated bridging ligands of the back-to-back dinuclear platinum complexes has not been reported yet.

To remedy this deficiency, we have designed and synthesized a series of novel dinuclear platinum(II) complexes with different substituents on the bridging ligand (**1a–1d**, Chart 1). Br and CN were selected as the electron-withdrawing groups and  $\text{OC}_{12}\text{H}_{25}$  was chosen as electron-donating substituent. The *tert*-butyl groups were introduced on the terpyridine ligands in order to increase the solubility of the target complexes and avoid the  $\pi$ – $\pi$  stack between the neighboring molecules. The photophysical properties of these complexes were systematically investigated with the aim of understanding the structure–property correlations and developing novel broadband nonlinear transmission materials. The synthetic routes are illustrated in Scheme 1.

\* Corresponding author. Tel.: +1 701 231 6254; fax: +1 701 231 8831.

E-mail address: [Wenfang.Sun@ndsu.edu](mailto:Wenfang.Sun@ndsu.edu) (W. Sun).

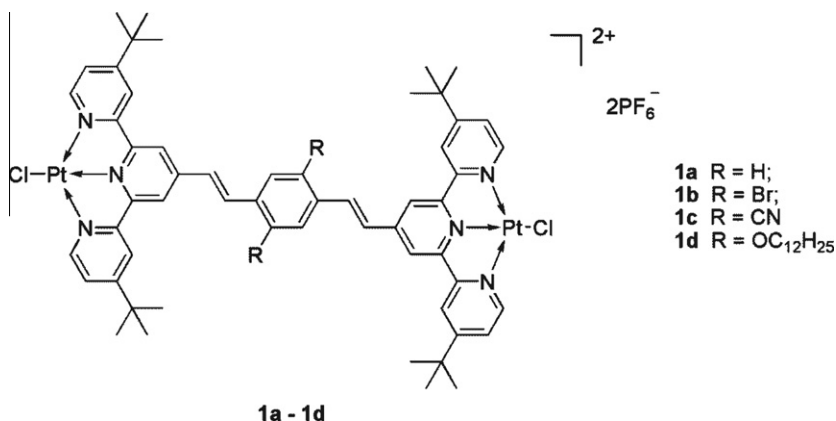


**Chart 1.** Molecule structures of dinuclear Pt(II) complexes **1a–1d**.

## 2. Experimental

### 2.1. Materials

All of the chemicals and solvents were purchased from Alfa Aesar and used as is unless otherwise stated. 4-*Tert*-butyl-2-acetylpyridine (**9**) [20], 1-(4-*tert*-butylpyridin-2-yl)-3-hydroxybutan-1-one (**8**) [21], 1-(4-*tert*-butylpyridin-2-yl)but-2-en-1-one (**7**) [21], 4,4''-bis-*tert*-butyl-4'-methyl-2,2':6',2''-terpyridine (**6**) [21,22], 4,4''-bis-*tert*-butyl-4'-formyl-2,2':6',2''-terpyridine (**5**) [23,24], 1,4-bis(bromomethyl)benzene derivatives (**4a–4d**) [25–28], tetraethyl-[1,4-phenylenbis(methylen)]-bisphosphonate (**3a–3d**) [25,28–30] and terpyridine ligands (**2a–2d**) [29,31–33] were all synthesized according to the literature procedures. Column chromatography was carried out using silica gel (Sorbent Technologies, 60 Å, 230 × 400 mesh) or neutral aluminum oxide (Sigma–Aldrich, 58 Å, ~150 mesh).

### 2.2. Measurements

<sup>1</sup>H NMR spectra were recorded on either a Bruker AV-400 or AV-500 spectrometer using DMSO-*d*<sub>6</sub> as the solvent, with tetramethylsilane (TMS) as internal standard. Elemental analyses were conducted by NuMega Resonance Laboratories, Inc., San Diego, CA. High resolution mass (HRMS) analyses were performed at Bruker BioTof III mass spectrometer. UV–Vis absorption spectra were obtained by using an Agilent 8453 spectrophotometer. Emission spectra were carried out on a SPEX fluorolog-3 fluorometer/phosphorometer. The emission quantum yields were determined by the comparative method [34], in which a degassed aqueous solution of [Ru(bpy)<sub>3</sub>]Cl<sub>2</sub> ( $\Phi_{em} = 0.042$ , excited at 436 nm) [35] was used as the reference. An Edinburgh LP920 laser flash photolysis spectrometer was used to acquire the triplet transient difference absorption (TA) spectra in degassed solutions. The excitation source was the third harmonic output (355 nm) of a Nd:YAG laser (Quantel Brilliant, pulsewidth ~4.1 ns, repetition rate was set at 1 Hz). Each sample was purged with Ar for 30 min prior to measurement.

The triplet excited-state molar extinction coefficients ( $\epsilon_T$ ) at the TA band maximum were determined by the singlet depletion method [36], in which the following equation was used to calculate the  $\epsilon_T$  [36].

$$\epsilon_T = \frac{\epsilon_S[\Delta OD_T]}{\Delta OD_S}$$

where  $\Delta OD_S$  and  $\Delta OD_T$  are the optical density changes at the minimum of the bleaching band and at the maximum of the positive

band in the TA spectrum, respectively, and  $\epsilon_S$  is the ground-state molar extinction coefficient at the wavelength of the bleaching band minimum. The triplet excited-state quantum yield ( $\Phi_T$ ) was obtained by relative actinometry [37], and SiNC in benzene was used as the reference ( $\epsilon_{590} = 70\,000\text{ M}^{-1}\text{ cm}^{-1}$ ,  $\Phi_T = 0.20$ ) [38].

### 2.3. Synthesis

#### 2.3.1. General procedure for synthesis of complexes **1a–1d**

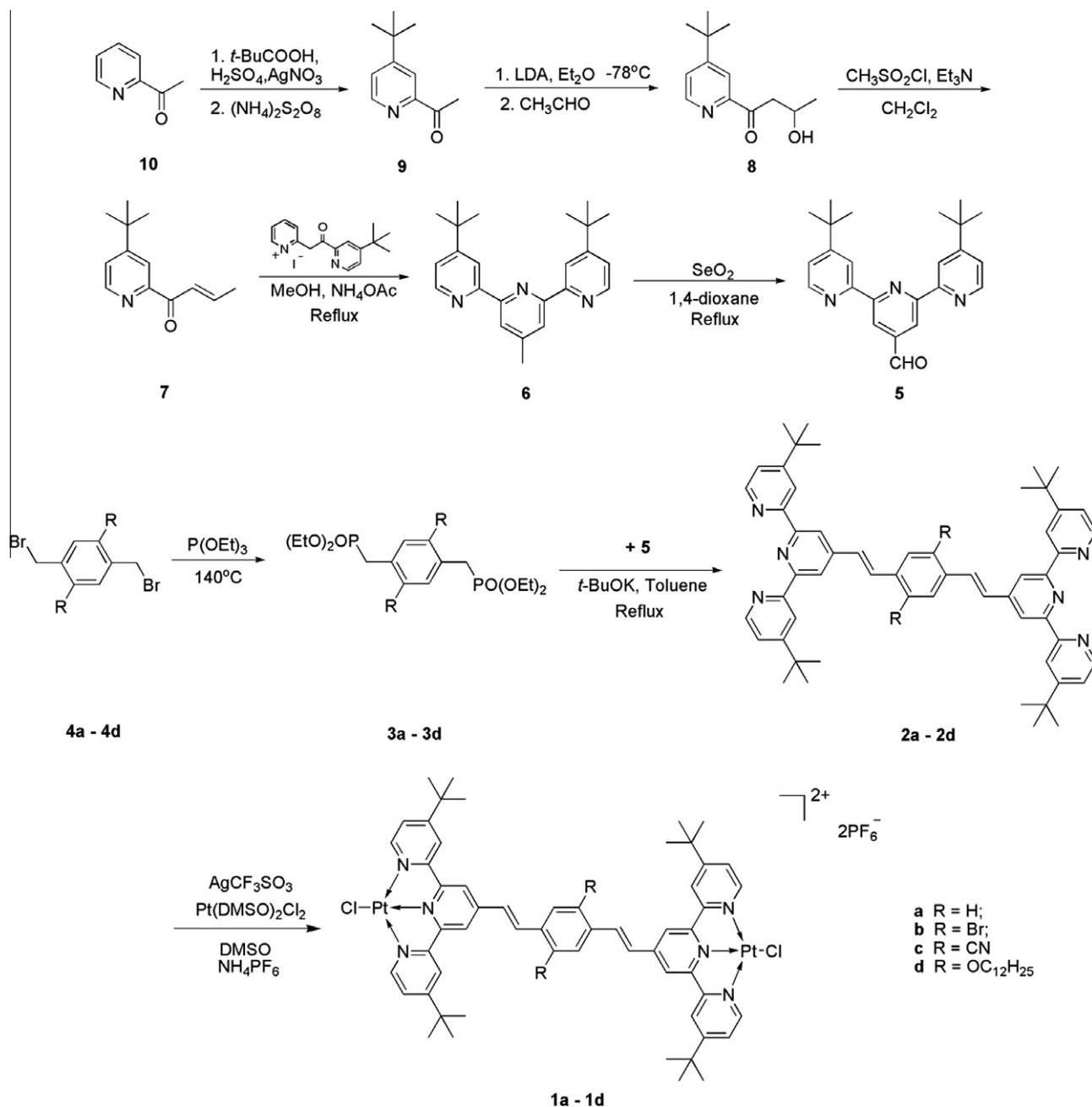
Pt(DMSO)<sub>2</sub>Cl<sub>2</sub> (260 mg, 0.6 mmol) and AgCF<sub>3</sub>SO<sub>3</sub> (160 mg, 0.6 mmol) were added in 5 mL of dimethylsulfoxide (DMSO). The mixture was stirred at room temperature for 24 h, and the white solid was filtered out. The filtrate was heated to 80 °C, and terpyridine ligands (**2a–2d**) (0.3 mmol) was added. The mixture was kept at 80 °C for 2 h. After cooling to room temperature, excess amount of saturated NH<sub>4</sub>PF<sub>6</sub> aqueous solution was added. The mixture was stirred at room temperature for 1 h, and the solid was collected by centrifugation. Then the solid was purified by recrystallization from DMF/ether to afford the desired product.

Complex **1a** (yield: 44%) as orange solid. <sup>1</sup>H NMR (400 MHz, CDCl<sub>3</sub>):  $\delta$  8.98 (s, 4H), 8.79 (d,  $J = 6.0$  Hz, 4H), 8.56 (s, 4H), 8.03–7.88 (m, 10H), 7.49 (d,  $J = 16.0$  Hz, 2H), 1.42 (s, 36H). HRMS ( $m/z$ ): calcd for [C<sub>56</sub>H<sub>60</sub>N<sub>6</sub>Cl<sub>2</sub>Pt<sub>2</sub>]<sup>2+</sup>, 638.6768; found, 638.6743 (100%). Anal. Calc. for C<sub>56</sub>H<sub>60</sub>N<sub>6</sub>Cl<sub>2</sub>P<sub>2</sub>F<sub>12</sub>Pt<sub>2</sub>·CH<sub>2</sub>Cl<sub>2</sub>: C, 41.41; H, 3.78; N, 5.10. Found: C, 41.75; H, 3.90; N, 5.58%.

Complex **1b** (yield: 57%) as yellow solid. <sup>1</sup>H NMR (400 MHz, CDCl<sub>3</sub>):  $\delta$  8.98 (s, 4H), 8.79 (d,  $J = 6.0$  Hz, 4H), 8.36 (s, 4H), 8.27 (s, 2H), 8.00 (d,  $J = 16.0$  Hz, 2H), 7.95 (dd,  $J = 6.0$  Hz,  $J = 2.0$  Hz, 4H), 7.49 (d,  $J = 16.0$  Hz, 2H), 1.42 (s, 36H). HRMS ( $m/z$ ): calcd for [C<sub>56</sub>H<sub>58</sub>N<sub>6</sub>Br<sub>2</sub>Cl<sub>2</sub>Pt<sub>2</sub>]<sup>2+</sup>, 718.0862; found, 718.0880 (100%). Anal. Calc. for C<sub>56</sub>H<sub>58</sub>N<sub>6</sub>Br<sub>2</sub>Cl<sub>2</sub>P<sub>2</sub>F<sub>12</sub>Pt<sub>2</sub>·DMF: C, 36.73; H, 3.40; N, 4.96. Found: C, 36.42; H, 3.40; N, 5.33%.

Complex **1c** (yield: 48%) as yellow solid. <sup>1</sup>H NMR (400 MHz, CDCl<sub>3</sub>):  $\delta$  9.00 (s, 4H), 8.85 (d,  $J = 6.0$  Hz, 4H), 8.61 (s, 4H), 8.06–7.93 (m, 6H), 7.77 (d,  $J = 16.0$  Hz, 2H), 1.42 (s, 36H). HRMS ( $m/z$ ): calcd for [C<sub>58</sub>H<sub>58</sub>N<sub>8</sub>Cl<sub>2</sub>Pt<sub>2</sub>]<sup>2+</sup>, 633.6720; found, 633.6734 (100%). Anal. Calc. for C<sub>58</sub>H<sub>58</sub>N<sub>8</sub>Cl<sub>2</sub>P<sub>2</sub>F<sub>12</sub>Pt<sub>2</sub>·<sup>1</sup>/<sub>3</sub>DMF·CH<sub>2</sub>Cl<sub>2</sub>: C, 41.71; H, 3.67; N, 6.75. Found: C, 41.63; H, 3.73; N, 7.14%.

Complex **1d** (yield: 54%) as black solid. <sup>1</sup>H NMR (400 MHz, CDCl<sub>3</sub>):  $\delta$  8.92 (s, 4H), 8.83 (d,  $J = 6.0$  Hz, 4H), 8.63 (d,  $J = 2.0$  Hz, 4H), 8.14 (d,  $J = 16.0$  Hz, 2H), 8.63 (d,  $J = 2.0$  Hz, 4H), 7.53 (dd,  $J = 2.0$  Hz,  $J = 6.0$  Hz, 2H), 7.50 (s, 2H), 4.17 (t,  $J = 5.8$  Hz, 4H), 1.88–1.85 (m, 2H), 1.52–1.49 (m, 2H), 1.38–1.32 (m, 4H), 1.42 (s, 36H), 1.21–0.98 (m, 32H), 0.72 (t,  $J = 7.2$  Hz, 6H). HRMS ( $m/z$ ): calcd for [C<sub>80</sub>H<sub>108</sub>N<sub>6</sub>Cl<sub>2</sub>O<sub>2</sub>Pt<sub>2</sub>]<sup>2+</sup>, 823.3600; found, 823.3601 (100%). Anal. Calc. for C<sub>80</sub>H<sub>108</sub>N<sub>6</sub>Cl<sub>2</sub>O<sub>2</sub>P<sub>2</sub>F<sub>12</sub>Pt<sub>2</sub>·<sup>1</sup>/<sub>2</sub>DMF: C, 48.99; H, 5.70; N, 4.61. Found: C, 48.70; H, 5.32; N, 4.83%.

Scheme 1. Synthetic routes for complexes **1a-1d**.

### 3. Results and discussion

#### 3.1. Synthesis

The synthetic routes for **1a-1d** are shown in Scheme 1. Four *tert*-butyl substituents were introduced to the terpyridine components in order to reduce the intermolecular  $\pi$ - $\pi$  stacking and thus improve the solubility of the Pt(II) complexes. Ligands **2a-2d** were prepared by the Wittig-Horner reaction between the bis-phosphonate (**3a-3d**) and the formyl-functionalized terpyridine (**5**), with *t*-BuOK as the base [29,31–33].

Coordination reactions of the target complexes (**1a-1d**) were carried out via the procedure reported previously [12]. A highly reactive platinum salt was prepared by exchange of one of the chloride coligands in  $Pt(DMSO)_2Cl_2$  with 1 equiv. of  $CF_3SO_3^-$  anion

from  $AgCF_3SO_3$  in DMSO. After filtration of AgCl, one-half molar equivalent of terpyridine ligand (**2a-2d**) was added to the filtrate and the reaction solution was heated to 80 °C for 2 h. Pure final product was obtained in 58–68% yield after recrystallization from DMF/Et<sub>2</sub>O. All the synthesized complexes were characterized by <sup>1</sup>H NMR, HRMS, and elemental analysis.

#### 3.2. UV-Vis absorption

The UV-Vis absorption spectra of complexes **1a-1d** in CH<sub>3</sub>CN solution are presented in Fig. 1, and the absorption band maxima and the extinction coefficients are listed in Table 1. The UV-Vis absorption obeys Lambert-Beer's law in the concentration range of  $1 \times 10^{-6}$ – $1 \times 10^{-4}$  mol/L, suggesting that no ground-state aggregation occurs in this concentration range. The absorption

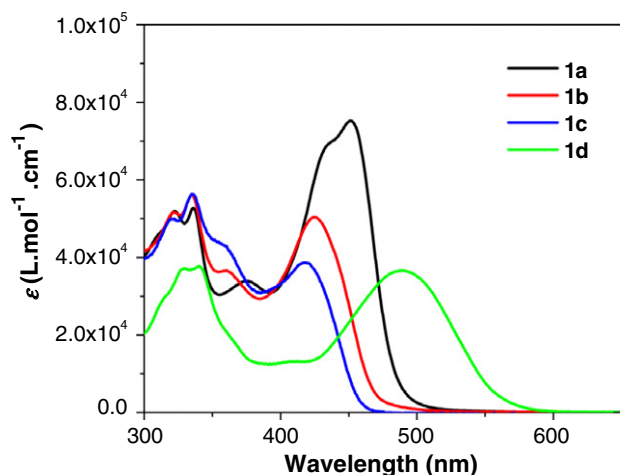


Fig. 1. UV-Vis absorption spectra of complexes **1a–1d** in  $\text{CH}_3\text{CN}$  solution.

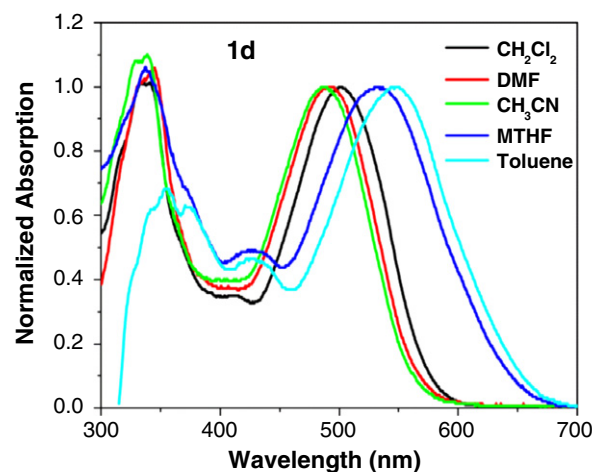


Fig. 3. Normalized UV-Vis absorption spectra of **1d** in different solvents.

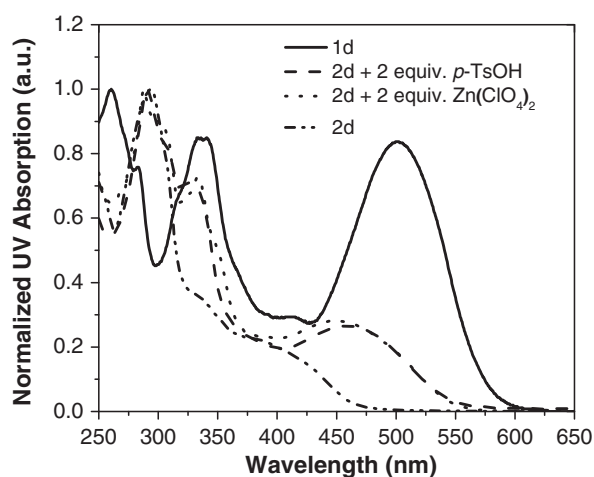


Fig. 2. Comparison of UV-Vis spectra of Pt complex **1d**, ligand **2d**, and **2d** with 2 equivalents of *p*-TsOH or  $\text{Zn}(\text{ClO}_4)_2$  in  $\text{CH}_2\text{Cl}_2$ .

spectra of **1a–1d** show strong intraligand (IL)  $^1\pi,\pi^*$  transitions in the UV region, which is in line with our previous work on “back-to-back” dinuclear platinum(II) terpyridine complexes [12] and with that of dinuclear ruthenium diimine complexes [39,40]. In addition, a broad, intense absorption band appears at 400–600 nm. With reference to that reported for dinuclear ruthenium complexes with similar bridging ligands, this absorption band could be tentatively assigned to the  $^1\text{MLCT}$  (metal-to-bridging ligand charge transfer) transition. Similar to that observed in dinuclear Ru complexes with similar bridging ligand, the molar

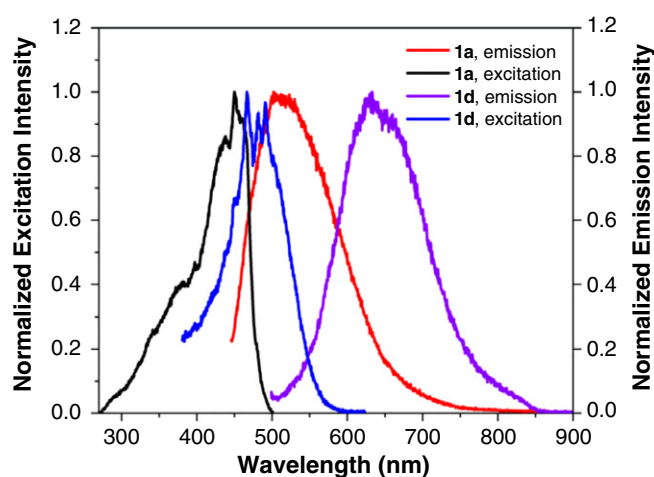


Fig. 4. Normalized emission spectra of **1a** and **1d** in  $\text{CH}_3\text{CN}$  solution ( $1 \times 10^{-5}$  mol/L). The excitation wavelength was 450 nm for **1a** and 488 nm for **1d**.

extinction coefficient of this  $^1\text{MLCT}$  band is much higher than those of the typical  $^1\text{MLCT}$  transition in mononuclear Pt complexes. This should arise from the large transition dipole of the  $\text{Pt}(d\pi) \rightarrow \text{tpy}(\text{dvbtpy})(\pi^*)$  (dvb refers to divinylbenzene linker and tpy refers to terpyridine) due to the extended conjugation in the bridging ligand. On the other hand, this band could have some contributions from the intraligand charge transfer ( $^1\text{ILCT}$ ) transition from the dvb linker to the terpyridine components. This notion is supported by the appearance of the intramolecular charge transfer ( $^1\text{ICT}$ ) band at ca. 460 nm upon acid or  $\text{Zn}^{2+}$  titration of the

**Table 1**  
Photophysical parameters of **1a–1d** in  $\text{CH}_3\text{CN}$ .<sup>a</sup>

	$\lambda_{\text{abs}}^b/\text{nm}$ ( $\epsilon/10^3 \text{ L mol}^{-1} \text{ cm}^{-1}$ )	$\lambda_{\text{em}}^b/\text{nm}$ ( $\tau_{\text{em}}/\text{ns}$ ; $\Phi_{\text{em}}$ )	$\lambda_{\text{T1-Tn}}/\text{nm}$ ( $\tau_{\text{TA}}/\text{ns}$ ; $\epsilon_{\text{T1-Tn}}/10^3 \text{ L mol}^{-1} \text{ cm}^{-1}$ ; $\Phi_{\text{T}}^d$ )
<b>1a</b>	256 (64.7), 335 (52.4), 450 (75.0)	527 (3.2; (41%), 0.32 (59%); 0.02)	700 (1550; 123200; 0.15)
<b>1b</b>	258 (65.4), 334 (55.9), 424 (50.3)	c	685 (190; 54200; 0.17)
<b>1c</b>	257 (71.5), 335 (56.3), 418 (38.6)	c	660 (160; 175200; 0.09)
<b>1d</b>	258 (43.7), 340 (37.7), 488 (36.6)	631 (3.7 (5%), 0.23 (95%); 0.003)	745 (1630; 31800; 0.21)

<sup>a</sup> Measured at room temperature.

<sup>b</sup> At a concentration of  $1 \times 10^{-5}$  mol/L.

<sup>c</sup> Too weak to be measured.

<sup>d</sup> Nanosecond TA band maximum, triplet extinction coefficient, triplet excited-state lifetime, and quantum yield. SiNc in  $\text{C}_6\text{H}_6$  was used as the reference. ( $\epsilon_{590} = 70000 \text{ L mol}^{-1} \text{ cm}^{-1}$ ,  $\Phi_{\text{T}} = 0.20$ ).

**Table 2**  
Emission energy and quantum yields of **1a–1d** in different solvents.

	$\lambda_{em}/nm$ ( $\Phi_{em}$ )				
	CH <sub>3</sub> CN	DMF	CH <sub>2</sub> Cl <sub>2</sub>	MTHF	Toluene
<b>1a</b>	527 (0.02)	540 (0.0096)	530 (0.012)	a	a
<b>1d</b>	618 (0.003)	a	621 (0.027)	631 (0.003)	638 (0.006)

<sup>a</sup> Signal too weak to be detected.

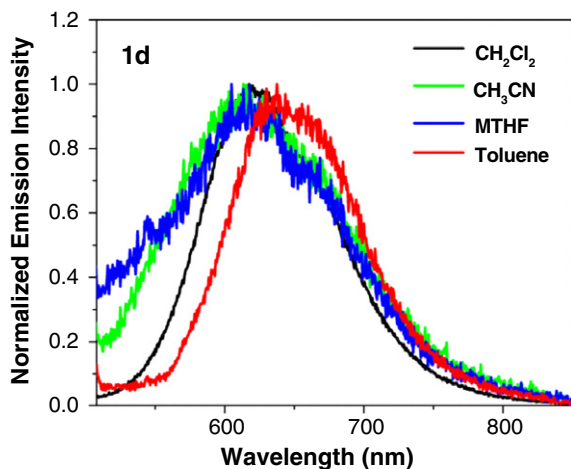


**Fig. 5.** Normalized emission spectra of **1d** in different solvents. The excitation wavelength was 436 nm.

respective 1,4-bis(terpyridin-4-yl-vinyl)benzene ligand, as exemplified in Fig. 2 for ligand **2d**, which is buried in the <sup>1</sup>MLCT band in **1d** and will be discussed in more detail later. Compared to the dinuclear Pt complex with 1,4-diethynyl-2,5-didodecyloxybenzene bridging ligand (complex **16** in reference [19]), the low-energy absorption band (<sup>1</sup>MLCT/<sup>1</sup>ILCT) of complex **1d** is red-shifted and the molar extinction coefficient is significantly increased. This phenomenon can be attributed to the better conjugation provided by the vinylene linker in the ligand than the ethynylene linker used for complex **16** due to the better  $\pi$ - $\pi$  and  $\pi^*$ - $\pi^*$  energy match at the C(sp<sup>2</sup>)-C(sp<sup>2</sup>) connections and the smaller bond length alternation for the double bond connection [41].

The charge transfer nature of the low-energy absorption band is clearly evident from the solvent-dependency UV-Vis study of these complexes. As exemplified in Fig. 3 for **1d**, the low-energy absorption band exhibits a negative solvatochromic effect (namely, in low polarity solvents, such as toluene, this band shows a bathochromic shift; whereas in more polar solvents, such as CH<sub>3</sub>CN, the band exhibits a hypsochromic shift), which is indicative of a charge-transfer transition. This phenomenon is in accordance with that observed in many of the platinum bipyridine or terpyridine complexes reported in the literature [11–13]. The same solvatochromic effect is observed for the other three complexes in this work, and the results are provided in Supporting information Figs. S1–S3.

In contrast to the intraligand <sup>1</sup> $\pi$ , $\pi^*$  transition band, the low-energy charge-transfer band is influenced significantly by the nature of the substituents on the bridging ligand. Electron-donating substituent, OC<sub>12</sub>H<sub>25</sub>, causes a pronounced red-shift of this transition, while electron-withdrawing substituents like Br and CN induce a blue-shift compared to that in complex **1a**. On one hand, this change is related to the effect of the substituent on the relative energy level of the Pt-based HOMO and bridging ligand based LUMO. A time-dependent density functional theory study of the molecular structure on the excited state polarizability of phenylenevinylene

oligomers revealed that there are strong couplings between the  $\pi$ -electron system on the phenylenevinylene backbone and orbitals on the OCH<sub>3</sub> and CN groups [42]. These interactions would alter the ligand field strength, which in turn influences the Pt-based HOMO. Electron-donating OC<sub>12</sub>H<sub>25</sub> substituent would increase the ligand field strength and consequently raises the Pt-based HOMO. Meanwhile, the bridging ligand based LUMO is also raised. However, the degree of the HOMO energy increase exceeds that of the LUMO, leading to a decrease of the HOMO-LUMO energy gap and the red-shift of the <sup>1</sup>MLCT band. In contrast, the electron withdrawing substituents, Br and CN, stabilize both the HOMO and LUMO. However, the HOMO is stabilized more than the LUMO, which causes the blue-shift of the <sup>1</sup>MLCT band. On the other hand, this substituent effect is also consistent with the nature of the intramolecular charge transfer transition. When electron-donating ability of the dvb linker increases, the ILCT from dvb to terpyridine is enhanced, which causes a red-shift of the charge-transfer band.

The mixture of <sup>1</sup>ILCT transition into the low-energy absorption band is further supported by the acid and Zn<sup>2+</sup> titration experiments of **2d**. As shown in Fig. 2 and Supporting information Fig. S4, upon addition of acids or Zn<sup>2+</sup>, the lowest-energy absorption band in **2d** red-shifts from 400 nm to ca. 460 nm, which is in close proximity to the charge-transfer band in **1d**. Due to the lack of metal center in acidified ligand and the absence of MLCT transition in the Zn complex, the new absorption band at ca. 460 nm should be attributed to the intramolecular charge transfer transition. After ligand complexation with Pt, electron density on the terpyridine components is reduced, which increases the electron-withdrawing ability of the terpyridine components, similar to the effect of protonation of the terpyridine component or complexation with the Zn<sup>2+</sup> ion. Therefore, intraligand charge transfer from the dvb component to the terpyridine components contributes to the low-energy charge transfer band in **1a–1d**. However, the ILCT contribution is strongest in **1d** that contains electron-donating -OC<sub>12</sub>H<sub>25</sub> substituent on the dvb linker, while the ILCT contribution is reduced in **1b** and **1c** that bear electron-withdrawing substituents on dvb. A similar assignment was reported for dinuclear Pt(II) complexes with  $\pi$ -donating fluorene as the bridging group [12].

### 3.3. Emission

The emission of complexes **1a–1d** in different solvents at room temperature was investigated. Only **1a** and **1d** exhibit structureless emission upon excitation at the low-energy absorption band. **1b**

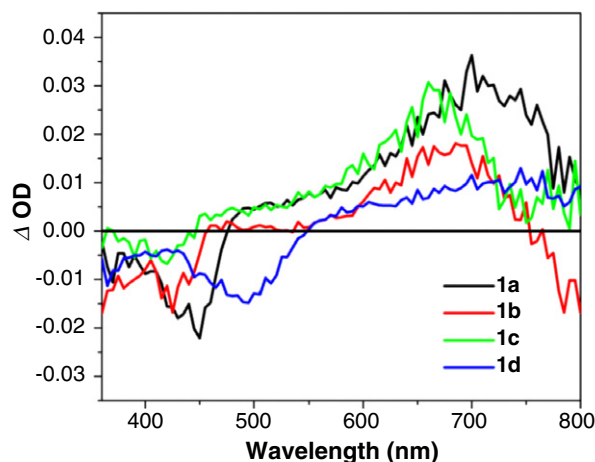


**Fig. 6.** Triplet transient difference absorption spectra of **1a–1d** at zero-delay after laser excitation in CH<sub>3</sub>CN solution.  $\lambda_{ex}$  = 355 nm.

and **1c** are nonemissive at room temperature in solution. The normalized emission spectra of **1a** and **1d** in CH<sub>3</sub>CN ( $1 \times 10^{-5}$  mol/L) along with their respective excitation spectra are illustrated in Fig. 4, and the emission quantum yields of these two complexes in different solvents are summarized in Table 2. The emission band maxima of **1a** and **1d** in CH<sub>3</sub>CN solution ( $\lambda_{\text{max}}$ ) appear at 527 and 631 nm, respectively; and the emission for both complexes exhibits biexponential decay, with a longer lifetime of  $\sim 3$  ns and a shorter one of hundreds of ps (listed in Table 1). In addition, the emission is insensitive to oxygen quenching. Both the emission intensity and lifetime remain the same in air-saturated solution and in deaerated solution (see Supporting information Fig. S5 for **1d**). The short lifetime along with the insensitivity to oxygen quenching imply that the observed emission is likely fluorescence from the <sup>1</sup>MLCT/<sup>1</sup>ILCT states. The charge-transfer nature of the emitting states is evident from the negative solvatochromic effect as exemplified in Fig. 5 for **1d** and in Supporting information Fig. S6 for **1a**. Compared to their respective ligands **2a** and **2d** (Supporting information Figs. S7, S8 and S11), the emission of the Pt(II) complexes exhibit significant red-shifts from 434 nm for **2a** to 527 nm for **1a**, and from 484 nm for **2d** to 631 nm for **1d**. This significant red-shift also reflects the charge-transfer nature of the emitting states in **1a** and **1d**, while the emitting states in the ligands are <sup>1</sup> $\pi, \pi^*$  state in nature. Our attribution of the emitting states in **1a** and **1d** to mixed <sup>1</sup>MLCT/<sup>1</sup>ILCT rather than a pure <sup>1</sup>ILCT or <sup>1</sup>MLCT state is based on the following three facts: first, as shown in Fig. 4, the emission bands of **1a** and **1d** exhibit mirror images to their low-energy <sup>1</sup>MLCT/<sup>1</sup>ILCT bands in UV–Vis spectra; secondly, acid and zinc titration study of ligand **2d** emission demonstrates that the emission band of ligand **2d** red-shifts from 475 to 528 nm upon addition of acids (Fig. S13) and to 562 nm upon addition of Zn(ClO<sub>4</sub>)<sub>2</sub> salts (Fig. S14), which are ascribed to the <sup>1</sup>ILCT state and are buried in the broad emission band of Pt complex **1d** at 631 nm. Considering the red-shift of the emission band in **1d** compared to the <sup>1</sup>ILCT emission in the acidified ligand **2d** or Zn-complexed **2d**, we believe that the observed emission at 631 nm for Pt complex **1d** is dominated by the <sup>1</sup>MLCT emission, but admixing with some <sup>1</sup>ILCT character. Thirdly, the emission of **1a** and **1d** exhibits biexponential decay, with the longer lifetime attributed to <sup>1</sup>ILCT and the shorter one to <sup>1</sup>MLCT. Furthermore, confirmation of the emission being from the singlet excited states rather than triplet excited states arises from the fact that the emission lifetimes of **1d** are shorter than those measured for the acidified **2d** (1.95 ns (22%) and 5.15 ns (78%)) and Zn-complexed **2d** (2.62 ns (55%) and 4.78 ns (45%)).

Similar to that observed in the UV–Vis absorption spectra, electron-donating substituent (OC<sub>12</sub>H<sub>25</sub>) causes a significant red-shift in emission. The lack of emission upon excitation at the charge transfer band in complexes **1b** and **1c** could be attributed to the increased energy of the <sup>1</sup>MLCT band due to the electron-withdrawing nature of the Br and CN substituents, which decreases the energy gap between the <sup>1</sup>MLCT state and the other high-lying but thermally accessible nonemissive state(s). As a result, no emission is observed from **1b** and **1c**. The lack of emission in **1b** and **1c** is also a reflection of weak ILCT in these two complexes due to the presence of electron-withdrawing substituent on the divb linker, which is verified by the acid-titration experiment for **2c** (Supporting information S12).

### 3.4. Transient difference absorption

In order to understand the triplet excited-state properties of **1a–1d**, the triplet transient absorption (TA) of these complexes in CH<sub>3</sub>CN was investigated. Fig. 6 displays the triplet transient difference absorption spectra of **1a–1d** at zero-time delay in degassed

CH<sub>3</sub>CN solution; and the triplet excited-state absorption coefficients, lifetimes and quantum yields are listed in Table 1.

The spectral features for **1a–1d** are similar, with a negative band below 550 nm and broad, structureless absorption bands in the visible to the NIR region. The absorption band is red-shifted for the complex with electron-donating substituents (**1d**) and blue-shifted for complexes with electron-withdrawing substituents (**1b** and **1c**) compared to **1a**, which is consistent with that observed in the UV–Vis absorption spectra. The negative bands occur at the similar positions as the charge-transfer absorption bands in their respective UV–Vis absorption spectra; thus, they should be ascribed to the bleaching of the ground state. The lifetimes monitored from the decay of the transient absorption at the band maxima for **1a–1d** vary from 160 ns to 1.6  $\mu$ s, which are drastically longer than the lifetimes obtained from the decay of emission. This indicates that the observed transient absorption originates from the triplet excited state. Considering the similar red to near-IR absorption band in the TA spectra of **1a–1d** to those reported in the literature for dinuclear Ru(II) or Re(I) complexes with same or similar divinylbenzene (dvb) bridging linker, we attribute the broad red to near-IR absorption band to bridging ligand localized triplet excited states (<sup>3</sup> $\pi, \pi$  or <sup>3</sup>ILCT) [39,40,43,44]. This assignment is also supported by the substituent effect at the dvb linker, which couples with the bridging ligand backbone and alters the electron density on the ligand. Consequently, the <sup>3</sup> $\pi, \pi$  or <sup>3</sup>ILCT energy is changed by the electron-donating or withdrawing nature of the substituent and the TA absorption band maximum is red- or blue-shifted.

## 4. Conclusions

Four dinuclear platinum complexes with substituted 1,4-bis(terpyridin-4-yl-vinyl)benzene ligand were synthesized and their photophysical properties were systematically investigated. The dinuclear platinum complexes show intense absorption in the visible region, which can be assigned as the <sup>1</sup>MLCT/<sup>1</sup>ILCT transitions. The <sup>1</sup>MLCT/<sup>1</sup>ILCT transition is influenced by the nature of the substituents on divinylbenzene linker. Electron-donating substituent causes a pronounced red-shift of this transition, while electron-withdrawing substituents (Br, CN) induce a blue-shift. The electron-withdrawing substituents also cause a quench of the emission. All the complexes exhibit broad absorption bands in their triplet transient difference absorption spectra, which are attributed to the bridging ligand localized triplet excited states (<sup>3</sup> $\pi, \pi$  or <sup>3</sup>ILCT). The transient absorption band maxima are also influenced by the substituents on the dvb linker, with a bathochromic shift for the complex with electron-donating substituents and a hypsochromic shift for the complexes with electron-withdrawing substituents. Therefore, the excited-state properties of the mono-metallic back-to-back dinuclear platinum complexes can be tuned via the alternation of the substituents on the bridging ligand.

## Acknowledgments

We would like to thank the National Science Foundation (CA-REER CHE-0449598) for financial support. We are grateful to Barry Pemberton at NDSU for measuring the emission lifetimes of **1a** and **1d**, and to Professor Sivaguru Jayaraman for valuable discussion.

## Appendix A. Supplementary material

The UV–Vis absorption spectra of **1a–1c** and the emission spectra of **1a** at room temperature in different solvents, the emission spectra of **1d** in air-saturated and degassed CH<sub>3</sub>CN solutions, the UV–Vis absorption and emission spectra of ligand **2d** in CH<sub>2</sub>Cl<sub>2</sub>

solution upon addition of *p*-TsOH or Zn(ClO<sub>4</sub>)<sub>2</sub>, the emission spectra of ligand **2a–2d** in different solvents, and the emission spectra of ligand **2c** in CH<sub>2</sub>Cl<sub>2</sub> solution upon addition of *p*-TsOH. Supplementary data associated with this article can be found, in the online version, at doi:10.1016/j.ica.2012.02.031.

## References

- [1] W. Lu, B.-X. Mi, M.C.W. Chan, Z. Hui, C.-M. Che, N. Zhu, S.-T. Lee, *J. Am. Chem. Soc.* 126 (2004) 4958.
- [2] W. Lu, B.-X. Mi, M.C.W. Chan, Z. Hui, N. Zhu, S.-T. Lee, C.-M. Che, *Chem. Commun.* (2002) 206.
- [3] D. Qiu, J. Wu, Z. Xie, Y. Cheng, L. Wang, *J. Organomet. Chem.* 694 (2009) 737.
- [4] V.W.-W. Yam, R.P.-L. Tang, K.M.-C. Wong, K.-K. Cheung, *Organometallics* 20 (2001) 4476.
- [5] Q. Wang, F. Xiong, F. Morlet-Savary, S. Li, Y. Li, J.-P. Fouassier, G. Yang, *J. Photochem. Photobiol.* 194 (2008) 230.
- [6] Z. Ji, Y. Li, W. Sun, *J. Organomet. Chem.* 694 (2009) 4140.
- [7] H. Zhang, B. Zhang, Y. Li, W. Sun, *Inorg. Chem.* 48 (2009) 3617.
- [8] P. Du, K. Knowles, R. Eisenberg, *J. Am. Chem. Soc.* 130 (2008) 12576.
- [9] P. Du, J. Schneider, P. Jarosz, R. Eisenberg, *J. Am. Chem. Soc.* 128 (2006) 7726.
- [10] P. Du, J. Schneider, P. Jarosz, J. Zhang, W.W. Brennessel, R. Eisenberg, *J. Phys. Chem. B* 111 (2007) 6887.
- [11] P. Shao, Y. Li, J. Yi, T.M. Pritchett, W. Sun, *Inorg. Chem.* 49 (2010) 4507.
- [12] Z. Ji, S. Li, Y. Li, W. Sun, *Inorg. Chem.* 49 (2010) 1337.
- [13] P. Shao, Y. Li, A. Azenkeng, M.R. Hoffmann, W. Sun, *Inorg. Chem.* 48 (2009) 2407.
- [14] Z. Ji, A. Azenkeng, M.R. Hoffmann, W. Sun, *Dalton Trans.* (2009) 7725.
- [15] J.A. Bailey, V.M. Miskowski, H.B. Gray, *Inorg. Chem.* 32 (1993) 369.
- [16] M. Utsuno, T. Yutaka, M. Murata, M. Kurihara, N. Tamai, H. Nishihara, *Inorg. Chem.* 46 (2007) 11291.
- [17] K.M.-C. Wong, N. Zhu, V.W.-W. Yam, *Chem. Commun.* (2006) 3441.
- [18] G. Lowe, A.S. Droz, T. Vilaivan, G.W. Weaver, J.J. Park, J.M. Pratt, L. Tweedale, L.R. Kelland, *J. Med. Chem.* 42 (1999) 3167.
- [19] R. Ziessel, S. Diring, *Tetrahedron Lett.* 47 (2006) 4687.
- [20] M.W. Cooke, P. Tremblay, G.S. Hanan, *Inorg. Chim. Acta* 361 (2008) 2259.
- [21] H. Wolpher, S. Sinha, J. Pan, A. Johansson, M.J. Lundqvist, P. Persson, R. Lomoth, J. Bergquist, L. Sun, V. Sundstrom, B. Akermark, T. Polivka, *Inorg. Chem.* 46 (2007) 638.
- [22] G.U. Priimov, P. Moore, P.K. Maritim, P.K. Butalanyi, N.W. Alcock, *J. Chem. Soc., Dalton Trans.* (2000) 445.
- [23] G.R. Newkome, H.W. Lee, *J. Am. Chem. Soc.* 105 (1983) 5956.
- [24] L. Flamigni, F. Barigelletti, N. Armaroli, J.-P. Collin, J.-P. Sauvage, J.A.G. Williams, *Chem. Eur. J.* 4 (1998) 1744.
- [25] C. Huang, J. Fan, X. Peng, Z. Lin, B. Guo, A. Ren, J. Cui, S. Sun, *J. Photochem. Photobiol.* 199 (2008) 144.
- [26] J.M. Lopez-Romero, R. Rico, R. Martinez-Mallorquin, J. Hierrezuelo, E. Guillen, C. Cai, J.C. Otero, I. Lopez-Tocon, *Tetrahedron Lett.* 48 (2007) 6075.
- [27] M.C. Bonifacio, C.R. Robertson, J.-Y. Jung, B.T. King, *J. Org. Chem.* 70 (2005) 8522.
- [28] J. Eldo, A. Ajayaghosh, *Chem. Mater.* 14 (2002) 410.
- [29] H. Li, S. Valiyaveetil, *Tetrahedron Lett.* 50 (2009) 5311.
- [30] L. Liu, M. Shao, X. Dong, X. Yu, Z. Liu, Z. He, Q. Wang, *Anal. Chem.* 80 (2008) 7735.
- [31] A. Winter, C. Friebe, M.D. Hager, U.S. Schubert, *Eur. J. Org. Chem.* 2009 (2009) 801.
- [32] N. Zhou, L. Wang, D.W. Thompson, Y. Zhao, *Org. Lett.* 10 (2008) 3001.
- [33] M.J. Plater, T. Jackson, *Tetrahedron* 59 (2003) 4673.
- [34] G.A. Crosby, J.N. Demas, *J. Phys. Chem.* 75 (1971) 991.
- [35] J. Van Houten, R.J. Watts, *J. Am. Chem. Soc.* 98 (1976) 4853.
- [36] I. Carmichael, G.L. Hug, *J. Phys. Chem. Ref. Data* 15 (1986) 1.
- [37] C.V. Kumar, L. Qin, P.K. Das, *J. Chem. Soc., Faraday Trans. 2* (80) (1984) 783.
- [38] P.A. Firey, W.E. Ford, J.R. Sounik, M.E. Kenney, M.A.J. Rodgers, *J. Am. Chem. Soc.* 110 (1988) 7626.
- [39] A.I. Baba, H.E. Ensley, R.H. Schmechl, *Inorg. Chem.* 34 (1995) 1198.
- [40] J.R. Shaw, R.T. Webb, R.H. Schmechl, *J. Am. Chem. Soc.* 112 (1990) 1117.
- [41] J.Q. Morley, *Int. J. Quantum Chem.* 46 (1993) 19.
- [42] F.C. Grozema, R. Telesca, J.G. Snijders, L.D.A. Siebbeles, *J. Chem. Phys.* 118 (2003) 9441.
- [43] X.-Y. Wang, A.D. Guerso, H. Tunuguntla, R.H. Schmechl, *Res. Chem. Intermed.* 33 (2007) 63.
- [44] J.R. Shaw, R.H. Schmechl, *J. Am. Chem. Soc.* 113 (1991) 389.